Photoinduced η pairing in the Kondo lattice model

Tomonori Shirakawa[1], Shohei Miyakoshi,[2] and Seiji Yunoki[1,2,3]

[1]*Computational Materials Science Research Team, RIKEN Center for Computational Science (R-CCS), Kobe, Hyogo 650-0047, Japan*
[2]*Computational Quantum Matter Research Team, RIKEN Center for Emergent Matter Science (CEMS), Wako, Saitama 351-0198, Japan*
[3]*Computational Condensed Matter Physics Laboratory, RIKEN Cluster for Pioneering Research (CPR), Wako, Saitama 351-0198, Japan*

The previous theoretical study has shown that pulse irradiation to the Mott insulating state in the Hubbard model can induce the enhancement of superconducting correlation due to the generation of η pairs [Kaneko *et al.,* Phys. Rev. Lett. **122**, 077002 (2019)]. Here, we show that the same mechanism can be applied to the Kondo lattice model, an effective model for heavy electron systems, by demonstrating that the pulse irradiation indeed enhances the η-pairing correlation. As in the case of the Hubbard model, the nonlinear optical process is essential to increase the number of photoinduced η pairs and thus the enhancement of the superconducting correlation. We also find the diffusive behavior of the spin dynamics after the pulse irradiation, suggesting that the increase of the number of η pairs leads to the decoupling between the conduction band and the localized spins in the Kondo lattice model, which is inseparably related to the photodoping effect.

I. INTRODUCTION

Recent extensive studies of photoinduced states of strongly correlated materials have paved the way to find new states of matter [1–3]. Indeed, they have observed many intriguing phenomena, including the photoinduced transient superconducting behavior [4–8] and the photoinduced insulator-to-metal transition [9–13]. These experimental observations have stimulated theoretical studies on nonequilibrium dynamics of strongly correlated electrons, mostly focusing on photoexcited states in Hubbard-like models [14–17].

In this context, we have previously studied a photoexcited state after pulse irradiation onto the Mott insulating state in the Hubbard model and found the strong enhancement of superconducting correlation due to η pairing [18], which is a pair density wave with phase π and is associated with the transverse components of pseudospin 1/2 operators, first introduced by C. N. Yang [19]. We have also shown that the η pairs are preferentially excited by the optical pulse field because of the selection rule forced by the symmetry of the η-pairing operators [18,20,21].

In this paper, we report that the same mechanism can be applied to another class of models, the Kondo lattice model, known as an effective model to describe electronic states in heavy electron systems [22,23]. The Kondo lattice model is composed of a conduction band with mobile electrons and localized spins coupled to each conduction site antiferromagnetically. Because the presence of the exchange interaction induces a nontrivial scattering between the mobile electrons and localized spins, the Kondo lattice model is studied in the context of many-body quantum systems [22].

We demonstrate numerically that the pulse irradiation onto the Kondo insulating ground state induces the enhancement of the η-pairing correlation. The enhancement of the η-pairing correlation is due to the increase of the number of η pairs that

are selectively generated by the pulse optical field because the Kondo lattice model possesses the pseudospin 1/2, i.e., η-SU(2), symmetry under which the current operator is a rank-1 tensor operator. This implies that a nonlinear optical process is essential to increase the number of η pairs and thus the enhancement of the superconducting correlation. Moreover, we find that the spin dynamics changes drastically and becomes diffusive after the pulse irradiation. This can be understood because the generation of η pairs by the pulse irradiation is equivalent to *in situ* doping of carriers for spin dynamics.

The rest of this paper is organized as follows. We first introduce the Kondo lattice model on a bipartite lattice and the η-pairing operators in Sec. II. We also explain how to introduce the pulse optical field into the model and discuss the effect with the time-dependent perturbation theory. We then show our numerical results in Sec. III and conclude this paper with a brief discussion in Sec. IV. The numerical details are supplemented in the Appendix.

II. η PAIRING IN KONDO LATTICE

In this section, we describe the η-pairing and the photoexcitation in the Kondo lattice model. We first introduce the Kondo lattice model on a bipartite lattice in Sec. II A. We next introduce the pseudospin 1/2 operators, i.e., η-pairing operators, defined for the Kondo lattice model in Sec. II B. We then show that the Kondo lattice model possesses the η-SU(2) symmetry and discuss its consequences. In Sec. II C, we introduce two kinds of tensor operators relevant to the photoexcitation process. We describe how to introduce the time-dependent field into the model in Sec. II D and analyze the effect with the time-dependent perturbation theory in Sec. II E.

A. Model

The Kondo lattice model is described by the following Hamiltonian:

$$\hat{\mathcal{H}} = \hat{\mathcal{H}}_t + \hat{\mathcal{H}}_J, \tag{1}$$

where

$$\hat{\mathcal{H}}_t = -t \sum_{\langle j, j' \rangle} \sum_{\sigma=\uparrow,\downarrow} (\hat{c}_{j\sigma}^\dagger \hat{c}_{j'\sigma} + \hat{c}_{j'\sigma}^\dagger \hat{c}_{j\sigma}) \tag{2}$$

and

$$\hat{\mathcal{H}}_J = J \sum_j \hat{\mathbf{S}}_j \cdot \hat{\mathbf{M}}_j. \tag{3}$$

Here $\hat{c}_{j\sigma}$ ($\hat{c}_{j\sigma}^\dagger$) denotes the annihilation (creation) operator of a mobile electron with spin σ ($=\uparrow, \downarrow$) at site j. The first sum in Eq. (2) indicated by $\langle j, j' \rangle$ runs over all pairs of nearest-neighbor sites j and j' in the lattice. We assume that the lattice is bipartite in which sites can be divided into two sublattices A and B such that there is no connection (i.e., bond) within the same sublattice. Namely, all nearest-neighbor sites j' of site $j \in A$ are $j' \in B$ and vice versa. We also assume that the numbers L_A and L_B of sites in sublattices A and B, respectively, are the same, i.e., $L_A = L_B = L/2$, where L is the number of sites in the whole lattice and is assumed to be even.

$\hat{\mathbf{S}}_j = (\hat{S}_j^x, \hat{S}_j^y, \hat{S}_j^z)$ in Eq. (3) denotes the spin operator of a mobile electron given by

$$\hat{S}_j^\mu = \tfrac{1}{2} \hat{\mathbf{c}}_j^\dagger \sigma_\mu \hat{\mathbf{c}}_j, \tag{4}$$

where

$$\hat{\mathbf{c}}_j^\dagger = (\hat{c}_{j\uparrow}^\dagger \quad \hat{c}_{j\downarrow}^\dagger), \tag{5}$$

$$\hat{\mathbf{c}}_j = \begin{pmatrix} \hat{c}_{j\uparrow} \\ \hat{c}_{j\downarrow} \end{pmatrix}, \tag{6}$$

and σ_μ ($\mu = x, y, z$) is the μ component of the Pauli matrix. $\hat{\mathbf{M}}_j = (\hat{M}_j^x, \hat{M}_j^y, \hat{M}_j^z)$ denotes the spin-1/2 operator for the localized spin at site j, which is coupled to the mobile electrons via the antiferromagnetic exchange interaction J (>0).

In this paper, we consider the half-filling case with the number of mobile electrons $N = L$. In this case, the ground state of the Kondo lattice model is insulating. However, the symmetry properties discussed in this section are not limited to the half-filling case and can be easily extended to the case away from half filling.

B. η-pairing operators for Kondo lattice model

C. N. Yang noticed that, in addition to the usual SU(2) rotational symmetry in the spin space, there exists an additional SU(2) pseudospin symmetry for the Hubbard model [19]. A similar symmetry structure is also found in the Kondo lattice model [22]. The pseudospin symmetry is described by the η-pairing operators defined as

$$\hat{\eta}_x = \frac{1}{2} \sum_j e^{i\phi_j} (\hat{c}_{j\uparrow}^\dagger \hat{c}_{j\downarrow}^\dagger + \hat{c}_{j\downarrow} \hat{c}_{j\uparrow}), \tag{7}$$

$$\hat{\eta}_y = \frac{1}{2i} \sum_j e^{i\phi_j} (\hat{c}_{j\uparrow}^\dagger \hat{c}_{j\downarrow}^\dagger - \hat{c}_{j\downarrow} \hat{c}_{j\uparrow}), \tag{8}$$

$$\hat{\eta}_z = \frac{1}{2} \sum_j (\hat{c}_{j\uparrow}^\dagger \hat{c}_{j\uparrow} + \hat{c}_{j\downarrow}^\dagger \hat{c}_{j\downarrow} - 1), \tag{9}$$

where ϕ_j is a phase factor given by

$$\phi_j = \begin{cases} 0 & (\mathrm{mod}\ 2\pi) & \text{for } j \in A \\ \pi & (\mathrm{mod}\ 2\pi) & \text{for } j \in B, \end{cases} \tag{10}$$

and hence $e^{i\phi_j} = e^{-i\phi_j} = 1$ or -1. The exact form of ϕ_j is determined once the geometry of the bipartite lattice is fixed. For example, for the two-dimensional square lattice, $\phi_j = \mathbf{q} \cdot \mathbf{r}_j$ with $\mathbf{q} = (\pi, \pi)$, where $\mathbf{r}_j$ indicates the position of site j in the lattice. It is easy to show that these η-pairing operators $\hat{\boldsymbol{\eta}} = (\hat{\eta}_x, \hat{\eta}_y, \hat{\eta}_z)$ satisfy the SU(2) commutation relations:

$$[\hat{\eta}_\mu, \hat{\eta}_\nu] = i \sum_\lambda \varepsilon_{\mu\nu\lambda} \hat{\eta}_\lambda \tag{11}$$

for $\mu, \nu, \lambda = x, y, z$, where $\varepsilon_{\mu\nu\lambda}$ is the Levi-Civita symbol.

We can also easily show that the η-pairing operators commute with the spin operators of mobile electrons, $\hat{\mathbf{S}}_j = (\hat{S}_j^x, \hat{S}_j^y, \hat{S}_j^z)$, i.e.,

$$[\hat{\eta}_\mu, \hat{S}_j^\mu] = 0, \tag{12}$$

as well as the kinetic part of the Hamiltonian, i.e.,

$$[\hat{\eta}_\mu, \hat{\mathcal{H}}_t] = 0. \tag{13}$$

Since the η-pairing operators also commute with the localized spins $\hat{\mathbf{M}}_j = (\hat{M}_j^x, \hat{M}_j^y, \hat{M}_j^z)$, we find that the η-pairing operators commute with the Hamiltonian:

$$[\hat{\eta}_\mu, \hat{\mathcal{H}}] = 0. \tag{14}$$

This implies that the Kondo lattice model is symmetric under the SU(2) pseudospin rotation, which is referred to as the η-SU(2) symmetry. Note that Eq. (14) is satisfied for all the components of η-pairing operators at any concentration of mobile electrons, while the corresponding commutation relations for the x and y components are fulfilled only at half filling for the Hubbard model [19].

In the Kondo lattice model, the total spin operators of mobile electrons,

$$\hat{S}_\mu = \sum_j \hat{S}_j^\mu, \tag{15}$$

for $\mu = x, y, z$ do not commute with the Hamiltonian but the total spin operators including the localized spin operators

$$\hat{S}_{\text{tot}}^\mu = \sum_j \left(\hat{S}_j^\mu + \hat{M}_j^\mu \right) \tag{16}$$

commute with the Hamiltonian $\hat{\mathcal{H}}$. The η-pairing operators characterize the symmetry related to the charge degrees of freedom, which is frozen for the localized spins in the Kondo lattice model.

Noticing that the total pseudospin operator squared that is defined as

$$\hat{\boldsymbol{\eta}}^2 = \hat{\eta}_x^2 + \hat{\eta}_y^2 + \hat{\eta}_z^2 \tag{17}$$

commutes with each component of the η-pairing operators,

$$[\hat{\eta}_\mu, \hat{\boldsymbol{\eta}}^2] = 0, \tag{18}$$

Eq. (14) suggests that we can block diagonalize an eigenstate of $\hat{\mathcal{H}}$ by quantum numbers (η, η_z) for operators $\hat{\boldsymbol{\eta}}^2$ and $\hat{\eta}_z$. Let $|n, \eta, \eta_z\rangle$ be a simultaneous eigenstate for $\hat{\mathcal{H}}$, $\hat{\boldsymbol{\eta}}^2$, and $\hat{\eta}_z$:

$$\hat{\mathcal{H}}|n, \eta, \eta_z\rangle = E_{n\eta}|n, \eta, \eta_z\rangle, \tag{19}$$

$$\hat{\boldsymbol{\eta}}^2|n, \eta, \eta_z\rangle = \eta(\eta + 1)|n, \eta, \eta_z\rangle, \tag{20}$$

$$\hat{\eta}_z|n, \eta, \eta_z\rangle = \eta_z|n, \eta, \eta_z\rangle. \tag{21}$$

Note here that an energy eigenvalue $E_{n\eta}$ is independent of η_z, unlike the case of the Hubbard model [19]. This is because of the fact that

$$[\hat{\eta}_\pm, \hat{\mathcal{H}}] = 0, \tag{22}$$

where

$$\hat{\eta}_\pm = \hat{\eta}_x \pm i\hat{\eta}_y, \tag{23}$$

i.e., $\hat{\eta}_+ = \sum_j e^{i\phi_j}\hat{c}_{j\uparrow}^\dagger \hat{c}_{j\downarrow}^\dagger$ and $\hat{\eta}_- = \sum_j e^{-i\phi_j}\hat{c}_{j\downarrow}\hat{c}_{j\uparrow}$, and thus $[\hat{\eta}_+, \hat{\eta}_-] = 2\hat{\eta}_z$.

A simple example of simultaneous eigenstates is the vacuum state of mobile electrons, corresponding to $(\eta, \eta_z) = (L/2, -L/2)$. Here, the vacuum state can be represented as

$$|\text{vac}\rangle \equiv |0\rangle_f \otimes |\boldsymbol{\sigma}\rangle_S, \tag{24}$$

where $|0\rangle_f$ indicates the vacuum of mobile electrons in the conduction band and $|\boldsymbol{\sigma}\rangle_S$ with

$$\boldsymbol{\sigma} = \{\sigma_1, \sigma_2, \ldots, \sigma_j, \ldots, \sigma_L\} \quad (\sigma_j = \pm 1/2) \tag{25}$$

denotes a spin configuration of the localized spins. Indeed, we can readily find that

$$\hat{\mathcal{H}}|\text{vac}\rangle = 0, \tag{26}$$

$$\hat{\boldsymbol{\eta}}^2|\text{vac}\rangle = \frac{L}{2}\left(\frac{L}{2} + 1\right)|\text{vac}\rangle, \tag{27}$$

$$\hat{\eta}_z|\text{vac}\rangle = -\frac{L}{2}|\text{vac}\rangle. \tag{28}$$

Therefore, we can conclude that

$$|\text{vac}\rangle = |n, L/2, -L/2\rangle, \tag{29}$$

where n can be used to label the states for different spin configurations $\boldsymbol{\sigma}$. Note that the vacuum states are macroscopically degenerate due to the spin configurations of the localized spins, and thus the localized spins behave paramagnetic with no effective interaction mediated via mobile electrons.

By applying the $\hat{\eta}_+$ operator sequentially onto $|\text{vac}\rangle$, we can obtain an energy eigenstate for the different number of mobile electrons,

$$(\hat{\eta}_+)^{N/2}|\text{vac}\rangle \propto |n, L/2, -L/2 + N/2\rangle, \tag{30}$$

which contains N mobile electrons in the conduction band. Since the energy is independent of η_z, the states with $\eta = L/2$ are degenerate macroscopically and paramagnetic. The state given in Eq. (30) can also be obtained by applying the number projection to a BCS-type wave function,

$$|n, L/2, -L/2 + N/2\rangle \propto \hat{\mathcal{P}}_N|\text{BCS}\rangle \tag{31}$$

with

$$|\text{BCS}\rangle = \exp[\hat{\eta}_+]|0\rangle_f \otimes |\boldsymbol{\sigma}\rangle_S, \tag{32}$$

where $\hat{\mathcal{P}}_N$ denotes the projection operator onto the subspace with N mobile electrons. It is now clear that the state given in Eq. (30) exhibits the off-diagonal long-range order characterized by the pair correlation function P_η given by

$$P_\eta = \frac{1}{L}\sum_{j,j'} e^{i(\phi_j - \phi_{j'})}\langle \hat{c}_{j\uparrow}^\dagger \hat{c}_{j\downarrow}^\dagger \hat{c}_{j'\downarrow}\hat{c}_{j'\uparrow}\rangle = \frac{1}{L}\langle \hat{\eta}_+\hat{\eta}_-\rangle, \tag{33}$$

where $\langle \cdots \rangle = \langle \psi| \cdots |\psi\rangle$ indicates the expectation value for a given state $|\psi\rangle$. We can easily verify that, for the state given in Eq. (30),

$$P_\eta = \frac{N(2L - N + 2)}{4L}. \tag{34}$$

This implies that $P_\eta \propto L$, provided that $N \propto L$ for $L \to \infty$, suggesting the long-range ordering. Finally, we note that these states are not the ground state but energetically higher for a given η_z. Thereby, these properties are usually masked by the thermal average [21].

C. Tensor operators

Next, let us explain the relation between the η-pairing operators and the current operator. To this end, we introduce the following set of operators:

$$\hat{\mathcal{J}}_\alpha^{(0)} = -it\sum_{\langle j,j'\rangle}\sum_{\sigma=\uparrow,\downarrow} d_{jj'}^\alpha(\hat{c}_{j\sigma}^\dagger \hat{c}_{j'\sigma} - \hat{c}_{j'\sigma}^\dagger \hat{c}_{j\sigma}), \tag{35}$$

$$\hat{\mathcal{J}}_\alpha^{(1)} = -\sqrt{2}it\sum_{\langle j,j'\rangle} e^{i\phi_j}d_{jj'}^\alpha(\hat{c}_{j\uparrow}^\dagger \hat{c}_{j'\downarrow}^\dagger + \hat{c}_{j'\uparrow}^\dagger \hat{c}_{j\downarrow}^\dagger), \tag{36}$$

$$\hat{\mathcal{J}}_\alpha^{(-1)} = -\sqrt{2}it\sum_{\langle j,j'\rangle} e^{i\phi_j}d_{jj'}^\alpha(\hat{c}_{j\downarrow}\hat{c}_{j'\uparrow} + \hat{c}_{j'\downarrow}\hat{c}_{j\uparrow}). \tag{37}$$

Here, $d_{jj'}^\alpha (= -d_{j'j}^\alpha)$ is a scalar and depends on sites j and j'. $d_{jj'}^\alpha$ can be chosen arbitrary as long as sites j and j' belong to different sublattices of a bipartite lattice, implying that $e^{i\phi_j} = -e^{i\phi_{j'}}$. A practical choice of $d_{jj'}^\alpha$ is

$$d_{jj'}^\alpha = (\boldsymbol{r}_j - \boldsymbol{r}_{j'}) \cdot \boldsymbol{e}_\alpha, \tag{38}$$

where $\boldsymbol{r}_j$ indicates the position of site j and $\boldsymbol{e}_\alpha$ denotes the unit vector pointing to an arbitrary direction α. In this case, $\hat{\mathcal{J}}_\alpha^{(0)}$ corresponds to the current operator for the α direction. Note that we define $\hat{\mathcal{J}}_\alpha^{(-1)}$ so as to satisfy $(\hat{\mathcal{J}}_\alpha^{(+1)})^\dagger = -\hat{\mathcal{J}}_\alpha^{(-1)}$. In this case, we can show that these three operators satisfy the following commutation relations:

$$\begin{aligned}[\hat{\eta}_\pm, \hat{\mathcal{J}}_\alpha^{(q)}] &= \sqrt{(1 \mp q)(1 \pm q + 1)}\hat{\mathcal{J}}_\alpha^{(q\pm 1)}, \\ [\hat{\eta}_z, \hat{\mathcal{J}}_\alpha^{(q)}] &= q\hat{\mathcal{J}}_\alpha^{(q)},\end{aligned} \tag{39}$$

for $q = -1, 0, 1$. These relations in Eqs. (39) suggest that the set of operators $\hat{\mathcal{J}}_\alpha^{(q)}$ is a rank-1 tensor operator for the pseudospin operators $\hat{\eta}_\mu$ ($\mu = x, y, z$).

We can use the Wigner-Eckert theorem to evaluate a matrix element of a tensor operator between two states $|n, \eta, \eta_z\rangle$ and $|n', \eta', \eta_z'\rangle$ [24]. The theory states that, given the qth component of a tensor operator $\hat{\mathcal{T}}_{kq}$ of rank k, there exists a constant $\langle n\eta||\hat{\mathcal{T}}_k||n'\eta'\rangle$, referred to as a reduced matrix element, such

that for all η_z, η_z', and q,

$$\langle n, \eta, \eta_z | \hat{\mathcal{T}}_{kq} | n', \eta', \eta_z' \rangle = \langle \eta' \eta_z' kq | \eta \eta_z \rangle \langle n\eta || \hat{\mathcal{T}}_k || n'\eta' \rangle, \quad (40)$$

where $\langle \eta' \eta_z' kq | \eta \eta_z \rangle$ is the Clebsch-Gordan coefficient and $\langle n\eta || \hat{\mathcal{T}}_k || n'\eta' \rangle$ is independent of η_z, η_z', and q. Therefore, there is a finite matrix element for the current operator $\hat{\mathcal{J}}_\alpha^{(0)}$ only when $\eta' = \eta \pm 1$ and η. As we shall show below, this selection rule is essential when we discuss the photoexcitation.

Next, let us introduce the following kinetic energy operator in the α direction:

$$\hat{\mathcal{K}}_\alpha^{(0)} = -t \sum_{\langle j,j' \rangle} b_{jj'}^\alpha (\hat{c}_{j\sigma}^\dagger \hat{c}_{j'\sigma} + \hat{c}_{j'\sigma}^\dagger \hat{c}_{j\sigma}), \quad (41)$$

where $b_{jj'}^\alpha (= b_{j'j}^\alpha)$ is a scalar and depends on sites j and j' belonging to different sublattices of a bipartite lattice. We can readily show that $\hat{\mathcal{K}}_\alpha^{(0)}$ commutes with the η-pairing operators,

$$[\hat{\eta}_\pm, \hat{\mathcal{K}}_\alpha^{(0)}] = 0,$$
$$[\hat{\eta}_z, \hat{\mathcal{K}}_\alpha^{(0)}] = 0, \quad (42)$$

suggesting that $\hat{\mathcal{K}}_\alpha^{(0)}$ is a rank-0 tensor operator for the pseudospin operators $\hat{\eta}_\mu$ ($\mu = x, y, z$). The kinetic term $\hat{\mathcal{H}}_t$ in the Hamiltonian $\hat{\mathcal{H}}$ corresponds to the case when $b_{jj'}^\alpha = 1$ and thus it is a tensor operator of rank 0.

D. Time-dependent electric field

We introduce a time-dependent external field via the Peierls substitution by replacing $\hat{\mathcal{H}}_t$ in Eq. (2) with $\hat{\mathcal{H}}_t(\tau)$ given by

$$\hat{\mathcal{H}}_t(\tau) = -t \sum_{\langle j,j' \rangle} \sum_{\sigma=\uparrow,\downarrow} \left(e^{iA_{jj'}(\tau)} \hat{c}_{j\sigma}^\dagger \hat{c}_{j'\sigma} + e^{iA_{j'j}(\tau)} \hat{c}_{j'\sigma}^\dagger \hat{c}_{j\sigma} \right), \quad (43)$$

where $A_{jj'}(\tau)$ is the vector potential as a function of time τ,

$$A_{jj'}(\tau) = A(\tau)(\mathbf{r}_j - \mathbf{r}_{j'}) \cdot \mathbf{e}_\alpha. \quad (44)$$

For simplicity, the light velocity, the elementary charge, the Planck's constant, and the lattice constant are set to 1. In this paper, we consider the pump pulse given by

$$A(\tau) = A_0 e^{-(\tau-\tau_c)^2/(2\tau_w^2)} \cos[\omega_p(\tau - \tau_c)], \quad (45)$$

with the amplitude A_0, frequency ω_p (>0), and pulse width τ_w centered at time τ_c. This implies that a time-dependent electric field is applied along the α direction.

E. Time-dependent perturbation theory

It is highly instructive to analyze the effect of the time-dependent external field introduced above by using the time-dependent perturbation theory. For this purpose, we should first notice that the Hamiltonian $\hat{\mathcal{H}}(\tau)$ with the time-dependent external field can be decomposed as

$$\hat{\mathcal{H}}(\tau) = \hat{\mathcal{H}}_t(\tau) + \hat{\mathcal{H}}_J$$
$$= \hat{\mathcal{H}} + \hat{\mathcal{K}}_\alpha^{(0)}(\tau) + \hat{\mathcal{J}}_\alpha^{(0)}(\tau), \quad (46)$$

where the two classes of perturbation terms are

$$\hat{\mathcal{K}}_\alpha^{(0)}(\tau) = -t \sum_{\langle j,j' \rangle} \sum_{\sigma=\uparrow,\downarrow} (\cos A_{jj'}(\tau) - 1)(\hat{c}_{j\sigma}^\dagger \hat{c}_{j'\sigma} + \hat{c}_{j'\sigma}^\dagger \hat{c}_{j\sigma}) \quad (47)$$

and

$$\hat{\mathcal{J}}_\alpha^{(0)}(\tau) = -it \sum_{\langle j,j' \rangle} \sum_{\sigma=\uparrow,\downarrow} \sin A_{jj'}(\tau)(\hat{c}_{j\sigma}^\dagger \hat{c}_{j'\sigma} - \hat{c}_{j'\sigma}^\dagger \hat{c}_{j\sigma}). \quad (48)$$

Since $\cos A_{jj'}(\tau)$ [$\sin A_{jj'}(\tau)$] is even (odd) under the exchange of j and j', $\hat{\mathcal{K}}_\alpha^{(0)}(\tau)$ is a form of the kinetic energy operator defined in Eq. (41) and thus a tensor operator of rank 0, while $\hat{\mathcal{J}}_\alpha^{(0)}(\tau)$ is a form of one of the three operators introduced in Eqs. (35)–(37) and thus a tensor operator of rank 1. This implies that the time-dependent external field can excite a state to other states with η different at most by 1 in each order of the perturbation.

To explore this more explicitly, let us analyze the effect of the time-dependent external field using the time-dependent perturbation theory in the limit of $\tau_w \to \infty$. Here we also set $\tau_c = 0$, for simplicity. The similar analysis has been described briefly in Supplemental Material of Ref. [18]. In the limit of $\tau_w \to \infty$, we can simply Fourier expand the τ-dependent parts of the perturbations $\hat{\mathcal{K}}_\alpha^{(0)}(\tau)$ and $\hat{\mathcal{J}}_\alpha^{(0)}(\tau)$ as

$$\cos A_{jj'}(\tau) - 1 = \sum_{n=-\infty}^{\infty} e^{-i2n\omega_p\tau} f_{jj'}^{(2n)},$$
$$\sin A_{jj'}(\tau) = \sum_{n=-\infty}^{\infty} e^{-i(2n+1)\omega_p\tau} g_{jj'}^{(2n+1)}, \quad (49)$$

where n is integer, and $f_{jj'}^{(n)}$ and $g_{jj'}^{(n)}$ are the Fourier coefficients given by

$$f_{jj'}^{(n)} = \frac{1}{2\pi} \int_{-\infty}^{\infty} d\tau \left(\cos A_{jj'}(\tau) - 1 \right) e^{in\omega_p\tau},$$
$$g_{jj'}^{(n)} = \frac{1}{2\pi} \int_{-\infty}^{\infty} d\tau \sin A_{jj'}(\tau) e^{in\omega_p\tau}. \quad (50)$$

Note that the integral can be performed explicitly and the results are represented by using the Bessel functions $J_n(x)$ [25] as follows:

$$f_{jj'}^{(2n)} = (-1)^n \left(J_{2n}(A_0 d_{jj'}^\alpha) - \delta_{n0} \right), \quad (51)$$

$$g_{jj'}^{(2n+1)} = (-1)^n J_{2n+1}(A_0 d_{jj'}^\alpha), \quad (52)$$

with $d_{jj'}^\alpha$ in Eq. (38) and $f_{jj'}^{(2n+1)} = g_{jj'}^{(2n)} = 0$. Using these Fourier expansions, we obtain

$$\hat{\mathcal{V}}(\tau) = \hat{\mathcal{K}}_\alpha^{(0)}(\tau) + \hat{\mathcal{J}}_\alpha^{(0)}(\tau) = \sum_{n=-\infty}^{\infty} e^{-in\omega_p\tau} \hat{\mathcal{V}}_n, \quad (53)$$

where

$$\hat{\mathcal{V}}_{2n} = -t \sum_{\langle j,j' \rangle} \sum_{\sigma=\uparrow,\downarrow} f_{jj'}^{(2n)}(\hat{c}_{j\sigma}^\dagger \hat{c}_{j'\sigma} + \hat{c}_{j'\sigma}^\dagger \hat{c}_{j\sigma}), \quad (54)$$

$$\hat{\mathcal{V}}_{2n+1} = -it \sum_{\langle j,j' \rangle} \sum_{\sigma=\uparrow,\downarrow} g_{jj'}^{(2n+1)}(\hat{c}_{j\sigma}^\dagger \hat{c}_{j'\sigma} - \hat{c}_{j'\sigma}^\dagger \hat{c}_{j\sigma}). \quad (55)$$

Since $f_{jj'}^{(2n)} = f_{j'j}^{(2n)}$ and $g_{jj'}^{(2n+1)} = -g_{j'j}^{(2n+1)}$, we find that the even terms $\hat{\mathcal{V}}_{2n}$ are rank-0 tensor operators and the odd terms $\hat{\mathcal{V}}_{2n+1}$ are rank-1 tensor operators [see Eqs. (35) and (41)].

The time-dependent wave function $|\psi(\tau)\rangle$ is generally expanded in terms of the eigenstates $|\psi_m\rangle$ of the unperturbed Hamiltonian $\hat{\mathcal{H}}$ with the energies E_m:

$$|\psi(\tau)\rangle = 2\pi i \sum_m c_m(\tau)|\psi_m\rangle, \qquad (56)$$

where $m = 0, 1, 2, \ldots$ and $|\psi_0\rangle$ corresponds to the ground state of $\hat{\mathcal{H}}$ with $E_0 < E_1 \leqslant E_2 \leqslant \ldots$, assuming that the ground state is not degenerate. In the perturbation theory, the coefficient $c_m(\tau)$ is expanded by the order k of the perturbation:

$$c_m(\tau) = \sum_{k=0}^{\infty} c_m^{(k)}(\tau), \qquad (57)$$

with the initial condition that $|\psi(\tau = -\infty)\rangle = |\psi_0\rangle$, i.e., $c_m^{(k=0)}(\tau = -\infty) = \frac{1}{2\pi i}\delta_{m0}$.

According to the time-dependent perturbation theory, $c_m^{(k)}(\tau)$ is given as

$$c_m^{(k)}(\tau) = \frac{(-i)^k}{2\pi i} \int_{-\infty}^{\tau} d\tau_k \cdots \int_{-\infty}^{\tau_3} d\tau_2 \int_{-\infty}^{\tau_2} d\tau_1 \sum_{m_{k-1}} \cdots$$
$$\times \sum_{m_2} \sum_{m_1} \langle\psi_m|\hat{\mathcal{V}}_I(\tau_k)|\psi_{m_{k-1}}\rangle \cdots$$
$$\times \langle\psi_{m_2}|\hat{\mathcal{V}}_I(\tau_2)|\psi_{m_1}\rangle \langle\psi_{m_1}|\hat{\mathcal{V}}_I(\tau_1)|\psi_0\rangle, \qquad (58)$$

where $\hat{\mathcal{V}}_I(t) = e^{i\hat{\mathcal{H}}t}\hat{\mathcal{V}}(t)e^{-i\hat{\mathcal{H}}t}$. Because of Eq. (53), we can find the explicit τ dependance of each matrix element as

$$\langle\psi_m|\hat{\mathcal{V}}_I(t)|\psi_{m'}\rangle = \sum_{n=-\infty}^{\infty} e^{i(E_m - E_{m'} - n\omega_p)\tau} \mathcal{V}_{m,m'}^{(n)} \qquad (59)$$

with

$$\mathcal{V}_{m,m'}^{(n)} = \langle\psi_m|\hat{\mathcal{V}}_n|\psi_{m'}\rangle. \qquad (60)$$

Therefore, taking $\tau \to \infty$, we obtain that

$$c_m^{(k=1)}(\infty) = -\sum_{n=-\infty}^{\infty} \mathcal{V}_{m,0}^{(n)}\delta(E_m - E_0 - n\omega_p), \qquad (61)$$

and for $k > 1$,

$$c_m^{(k)}(\infty) = (-1)^k \sum_{n_k=-\infty}^{\infty} \cdots \sum_{n_2=-\infty}^{\infty} \sum_{n_1=-\infty}^{\infty} \sum_{m_{k-1}} \cdots$$
$$\times \sum_{m_2} \sum_{m_1} \mathcal{V}_{m,m_{k-1}}^{(n_k)} \cdots \mathcal{V}_{m_2,m_1}^{(n_2)} \mathcal{V}_{m_1,0}^{(n_1)}$$
$$\times \prod_{k'=1}^{k-1} \frac{1}{E_{m_{k'}} - E_0 - \left(\sum_{\ell=1}^{k'} n_\ell\right)\omega_p - i\delta}$$
$$\times \delta\left(E_m - E_0 - \left(\sum_{\ell=1}^{k} n_\ell\right)\omega_p\right), \qquad (62)$$

where $\delta \to 0^+$ is a convergence factor.

Equation (58) suggests that the transition from the initial state $|\psi_0\rangle$ to the final state $|\psi_m\rangle$ occurs via the intermediate

states $|\psi_{m_{k'}}\rangle$ with $k' = 1, 2, \ldots, k-1$. These intermediate states (and also the final state) are generated by applying the perturbations sequentially represented by $\mathcal{V}_{m_{k'},m_{k'-1}}^{(n_{k'})}$ in Eq. (62), i.e, either by the rank-0 tensor operators when $n_{k'}$ is even or by the rank-1 tensor operators when $n_{k'}$ is odd. Therefore, this forces the selection rule for the transition between the two intermediate states $|\psi_{m_{k'-1}}\rangle$ and $|\psi_{m_{k'}}\rangle$: $\Delta\eta = \eta_{m_{k'}} - \eta_{m_{k'-1}} = 0$ when $n_{k'}$ is even and $\Delta\eta = \pm 1$ or 0 when $n_{k'}$ is odd, where $\eta_{m_{k'}}(\eta_{m_{k'}} + 1)$ is the eigenvalue of $\hat{\boldsymbol{\eta}}^2$ for $|\psi_{m_{k'}}\rangle$. The denominators in Eq. (62) suggests that the k'th intermediate state $|\psi_{m_{k'}}\rangle$ contributes most when

$$E_{m_{k'}} = E_0 + \left(\sum_{l=1}^{k'} n_l\right)\omega_p = E_{m_{k'-1}} + n_{k'}\omega_p, \qquad (63)$$

implying that the energy difference ΔE between the two intermediate states $|\psi_{m_{k'-1}}\rangle$ and $|\psi_{m_{k'}}\rangle$ is $\Delta E = E_{m_{k'}} - E_{m_{k'-1}} = n_{k'}\omega_p$. This is indeed the energy conservation condition obtained by the first-order perturbation theory with taking $|\psi_{m_{k'-1}}\rangle$ as the initial state [see Eq. (61)]. These rules are schematically summarized in Figs. 1(a) and 1(b).

The delta function in Eq. (62) determines the final state energy E_m exactly as

$$E_m = E_0 + \left(\sum_{l=1}^{k} n_l\right)\omega_p. \qquad (64)$$

Therefore, the final state energy E_m is larger than the initial ground state energy E_0 by (integer)$\times\omega_p$, also implying that $\sum_{l=1}^{k} n_l \geqslant 0$. Since the final state is generated by applying the perturbations k times through exciting the $k-1$ intermediate states, the same selection rule described above is also set to the final state and is schematically illustrated in Fig. 1(c).

At half filling when $\eta_z = 0$, the selection rule is more characteristic because there is an additional rule such that

$$\langle n, \eta, 0|\hat{\mathcal{V}}_{2n+1}|n', \eta, 0\rangle = 0, \qquad (65)$$

because the Clebsch-Gordan coefficient in Eq. (40) is

$$\langle\eta 010|\eta 0\rangle = 0, \qquad (66)$$

suggesting that the transitions between two states with the same η value by the rank-1 tensor operators $\hat{\mathcal{V}}_{2n+1}$ are prohibited [also see Fig. 1(a)]. An important consequence of this is that the final state with an odd (even) value of η is excited at the excitation energy (odd (even) integer)$\times\omega_p$, as schematically shown in Fig. 1(c). This is because the final state with an odd (even) value of η can be excited only by involving the rank-1 tensor operators odd (even) times.

III. NUMERICAL CALCULATIONS

We first describe briefly the numerical setting of the calculations and numerical techniques used here, followed by the numerical results.

A. Numerical setting and techniques

In what follows, we consider the one-dimensional (1D) periodic lattice composed of L sites with the antiferromagnetic exchange interaction. In this case, the 1D Kondo lattice model
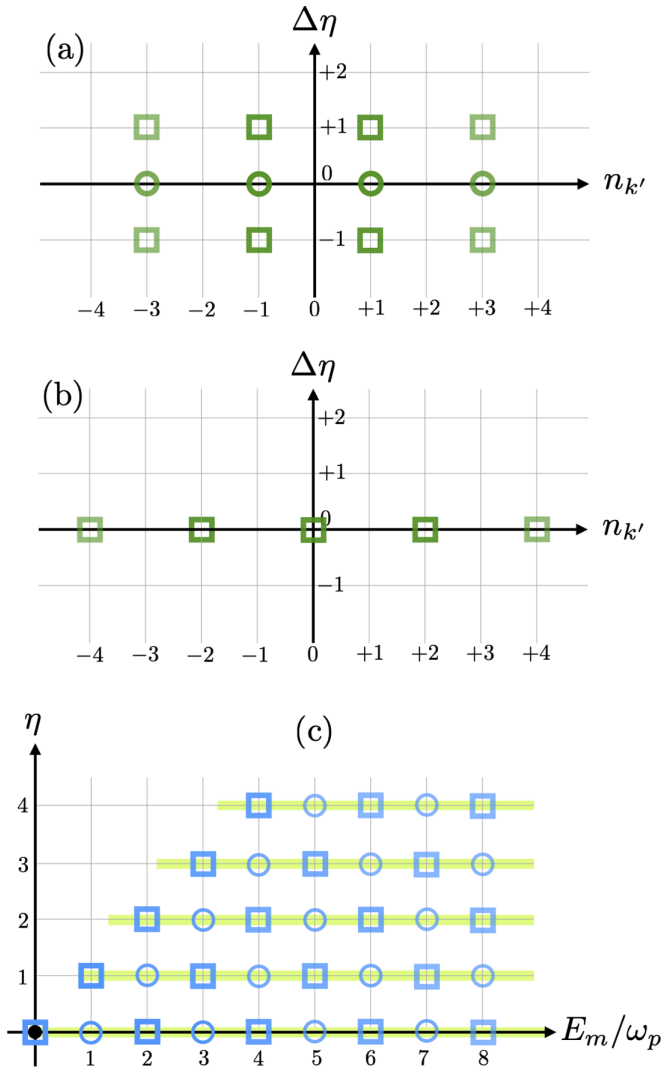
FIG. 1. Schematic figures of possible transition processes by (a) a rank-1 tensor operator and (b) a rank-0 tensor operator, and (c) possible distribution of eigenstates for the final state. In (a) and (b), the vertical axis is the quantum number difference $\Delta\eta$ and the horizontal axis is the energy difference ΔE in unit of ω_p (see the main text). Open green squares indicate transitions allowed in general while open green circles indicate transitions allowed only away from half filling. In (c), the vertical axis is the value of η and the horizontal axis is the energy E_m (in unit of ω_p) of eigenstates distributed in the final state. Here, we assume the energy distribution of the unperturbed Hamiltonian $\hat{\mathcal{H}}$ as indicated by light-green shaded bars. The initial ground state is indicated by a black solid circle. Open blue squares indicate eigenstates allowed in general while open blue circles indicate eigenstates allowed only away from half filling.

is described by the following Hamiltonian:

$$\hat{\mathcal{H}}(\tau) = \hat{\mathcal{H}}_t(\tau) + \hat{\mathcal{H}}_J,$$

$$\hat{\mathcal{H}}_t(\tau) = -t \sum_{j=1}^{L} \sum_{\sigma=\uparrow,\downarrow} (e^{-iA(\tau)} \hat{c}_{j\sigma}^{\dagger} \hat{c}_{j+1\sigma} + e^{iA(\tau)} \hat{c}_{j+1\sigma}^{\dagger} \hat{c}_{j\sigma}),$$

$$\hat{\mathcal{H}}_J = J \sum_{j=1}^{L} \hat{\mathbf{S}}_j \cdot \hat{\mathbf{M}}_j, \tag{67}$$

with $J > 0$ and $\hat{c}_{L+1\sigma} = \hat{c}_{1\sigma}$. At half filling ($N = L$), the ground state of this model with $A(\tau) = 0$ is an insulating state where both the spin and charge gaps open for any J/t [26–29]. The presence of the spin gap is attributed to the local singlet formation between the mobile electron and the localized spin via the finite exchange interaction J. Note that the finite spin gap suggests the finite correlation length of the antiferromagnetic correlation. This is sharp contrast to the two-dimensional case where there occurs the continuous quantum phase transition between the antiferromagnetically ordered and spin-gapped insulating phases with increasing J/t [30]. We, however, note that although the spin gap is finite, for small to moderate strength of the exchange interaction J, the antiferromagnetic correlation is dominant as compared to other correlations because of the small spin gap [29].

We employ the exact diagonalization technique to perform the time-dependent simulation. The initial state $|\psi(\tau = 0)\rangle$ is set to be the ground state of the Hamiltonian given in Eq. (67) with $A(\tau) = 0$. We obtain $|\psi(\tau = 0)\rangle$ by using the standard Lanczos technique. We then calculate the time-evolved state $|\psi(\tau)\rangle$ by applying the time-evolution operator with the small time step $\delta\tau$ sequentially:

$$|\psi(\tau + \delta\tau)\rangle = e^{-i\hat{\mathcal{H}}(\tau)\delta\tau}|\psi(\tau)\rangle. \tag{68}$$

To deal with the exponential form of the time-evolution operator, we simply use the Taylor expansion:

$$|\psi(\tau + \delta\tau)\rangle = \sum_{k=0}^{K} |v_k\rangle \tag{69}$$

with

$$|v_0\rangle = |\psi(\tau)\rangle,$$

$$|v_k\rangle = -\frac{i\delta\tau}{k} \hat{\mathcal{H}}(\tau)|v_{k-1}\rangle \quad \text{for } k \geqslant 1. \tag{70}$$

Note that, since the Hamiltonian is time dependent, one has to take the time step $\delta\tau$ small enough to reduce the systematic error, for which the Taylor expansion converges rather quickly. We set $\delta\tau = 0.01/t$ and determine K flexibly so as to satisfy $\langle v_K|v_K\rangle < 10^{-12}$. The results shown below are for $L = 8$ and $J = t$ at half filling.

B. Time evolution of correlation functions

Figure 2 shows typical results of the time dependence of several correlation functions. These correlation functions include the on-site pair correlation function,

$$\tilde{P}(q, \tau) = \frac{1}{L} \sum_{j=1}^{L} \sum_{j'=1}^{L} e^{-iq(j-j')} \langle \psi(\tau)|\hat{c}_{j\uparrow}^{\dagger} \hat{c}_{j\downarrow}^{\dagger} \hat{c}_{j'\downarrow} \hat{c}_{j'\uparrow}|\psi(\tau)\rangle, \tag{71}$$

the spin correlation function between mobile electrons,

$$\tilde{S}(q, \tau) = \frac{1}{L} \sum_{j=1}^{L} \sum_{j'=1}^{L} e^{-iq(j-j')} \langle \psi(\tau)|\hat{S}_j^z \hat{S}_{j'}^z|\psi(\tau)\rangle, \tag{72}$$

the spin correlation function between localized spins,

$$\tilde{M}(q, \tau) = \frac{1}{L} \sum_{j=1}^{L} \sum_{j'=1}^{L} e^{-iq(j-j')} \langle \psi(\tau)|\hat{M}_j^z \hat{M}_{j'}^z|\psi(\tau)\rangle, \tag{73}$$
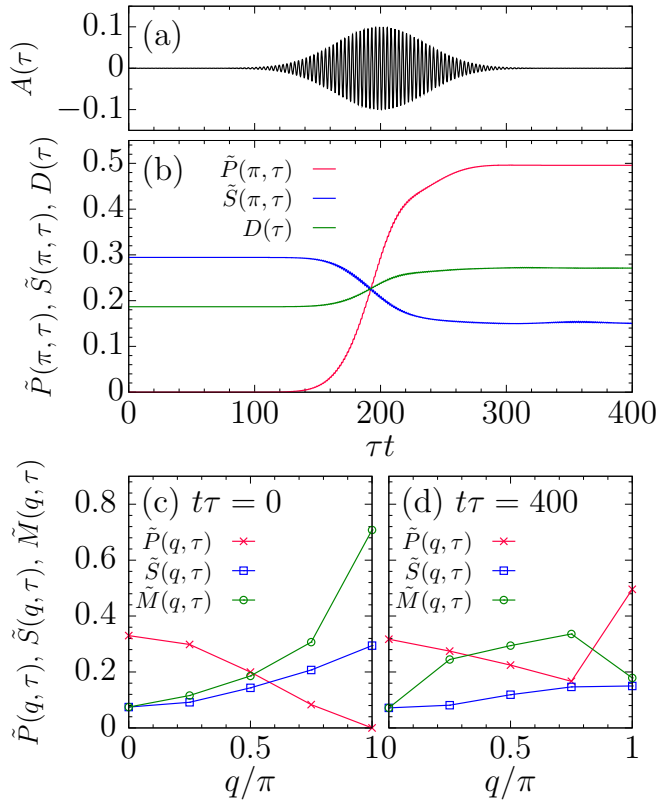
FIG. 2. (a) Time-dependent external field $A(\tau)$ used here with $A_0 = 0.1$, $\omega_p = 2.05t$, $\tau_c = 200/t$, and $\tau_w = 50/t$ [31]. (b) Time evolution of the on-site pair correlation function $\tilde{P}(q = \pi, \tau)$, the spin correlation function $\tilde{S}(q = \pi, \tau)$ for mobile electrons, and the double occupancy $D(\tau)$ for the 1D Kondo lattice model with $J = t$ and $L = 8$ at half filling. Momentum dependence of the on-site pair correlation function $\tilde{P}(q, \tau)$ and the spin correlation functions $\tilde{S}(q, \tau)$ and $\tilde{M}(q, \tau)$ at (c) $\tau = 0$ and (d) $\tau = 400/t$ for the same model parameters used in (b).

and the double occupancy,

$$D(\tau) = \frac{1}{L} \sum_{j=1}^{L} \langle \psi(\tau) | \hat{c}_{j\uparrow}^{\dagger} \hat{c}_{j\uparrow} \hat{c}_{j\downarrow}^{\dagger} \hat{c}_{j\downarrow} | \psi(\tau) \rangle. \quad (74)$$

Notice first that since $\hat{\mathcal{H}}(\tau)$ is spin SU(2) symmetric even when $A(\tau) \neq 0$, the spin correlation functions $\tilde{S}(q = 0, \tau)$ and $\tilde{M}(q = 0, \tau)$ defined above are exactly the same as those calculated for other spin components. Second, $\tilde{P}(q = \pi, \tau)$ corresponds to the correlation function for the η pairing because $\tilde{P}(q = \pi, \tau) = \frac{1}{L} \langle \psi(\tau) | \hat{\eta}^+ \hat{\eta}^- | \psi(\tau) \rangle = \frac{1}{L} \langle \psi(\tau) | (\hat{\eta}^2 - \hat{\eta}_z^2 + \hat{\eta}_z) | \psi(\tau) \rangle$. Third, $\tilde{S}(q = \pi, \tau)$ and $\tilde{M}(q = \pi, \tau)$ are the correlation functions for the antiferromagnetic ordering.

As shown in Figs. 2(b) and 2(c), the η-pairing correlation $\tilde{P}(q = \pi, \tau = 0)$ is exactly zero in the initial state. Since $\eta_z = 0$ at half filling, this implies that the initial state has $\eta = 0$. In contrast, the antiferromagnetic correlation is dominant in the initial state as we can observe in the correlation functions $\tilde{S}(q = \pi, \tau = 0)$ and $\tilde{M}(q = \pi, \tau = 0)$. We can also notice in Fig. 2(b) that the double occupancy $D(\tau = 0)$ in the initial state is around 0.18, much less than 0.25 expected for free electrons. The double occupancy is highly suppressed in
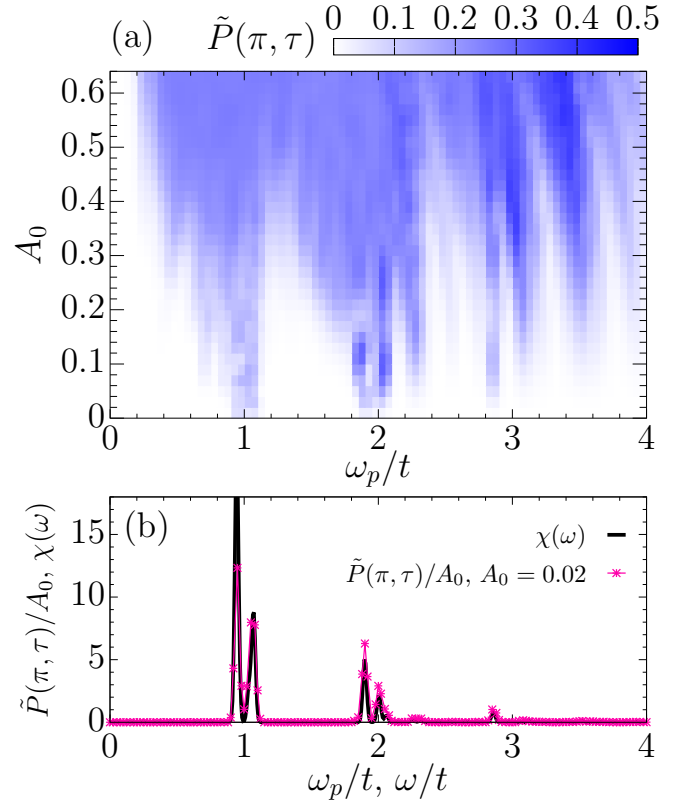

FIG. 3. (a) Contour plot of the on-site pair correlation function $\tilde{P}(q = \pi, \tau)$ at $\tau = 400/t$ with varying ω_p and A_0. (b) On-site pair correlation function $\tilde{P}(\pi, \tau = 400/t)$ as a function of ω_p for $A_0 = 0.02$ and dynamical current correlation function $\chi(\omega)$ for the initial ground state. ε in $\chi(\omega)$ is $0.01t$. The results are obtained for the 1D Kondo lattice model with $J = t$ and $L = 8$ at half filling. We use the external field $A(\tau)$ with $\tau_c = 200/t$ and $\tau_\omega = 50/t$.

the initial state because of the strong tendency toward the formation of local singlets. As the pulse is irradiated [also see Fig. 2(a)], the pair correlation function $\tilde{P}(q = \pi, \tau)$ [the spin correlation function $\tilde{S}(q = \pi, \tau)$] gradually increases (decreases), and by the time the pulse irradiation is terminated, the pair correlation function $\tilde{P}(q = \pi, \tau)$ becomes dominant [see Figs. 2(b) and 2(d)]. Note that the crossing of $\tilde{P}(q = \pi, \tau)$, $\tilde{S}(q = \pi, \tau)$, and $D(\tau)$ at $\tau = 200/t$ in Fig. 2(b) is simply accidental for this set of parameters.

To find the optimal parameter set for the enhancement of the η-pairing correlation, we show in Fig. 3(a) the contour plot of $\tilde{P}(q = \pi, \tau)$ after the pulse irradiation at $\tau = 400/t$ with different values of A_0 and ω_p. As shown in Fig. 3(b), for small A_0, we find that $\tilde{P}(\pi, \tau = 400/t)$ as a function of the frequencies ω_p almost coincides with the dynamical current correlation function $\chi(\omega)$ for the initial ground state $|\psi(0)\rangle = |\psi_0\rangle$ defined as

$$\chi(\omega) = \langle \psi(0) | \hat{\mathcal{J}} \delta_\varepsilon (\omega - \hat{\mathcal{H}} + E_0) \hat{\mathcal{J}} | \psi(0) \rangle, \quad (75)$$

where $\hat{\mathcal{J}}$ is the current operator given as

$$\hat{\mathcal{J}} = -it \sum_{j=1}^{L} \sum_{\sigma=\uparrow,\downarrow} (\hat{c}_{j\sigma}^{\dagger} \hat{c}_{j+1\sigma} - \hat{c}_{j+1\sigma}^{\dagger} \hat{c}_{j\sigma}) \quad (76)$$

and

$$\delta_\varepsilon(\hat{\mathcal{X}}) = \frac{1}{\sqrt{2\pi\varepsilon^2}} \exp[-\hat{\mathcal{X}}^2/2\varepsilon^2] \qquad (77)$$

for operator $\hat{\mathcal{X}}$, indicating that $\delta_\varepsilon(\hat{\mathcal{X}})$ approaches to the delta function in the limit of $\varepsilon \to 0^+$. We calculate $\chi(\omega)$ by using the method described in the Appendix. The coincidence of these two quantities is expected from the facts that $\hat{\mathcal{J}}|\psi(0)\rangle$ has to be a state with $\eta = 1$, because $\hat{\mathcal{J}}$ is a rank-1 tensor operator and the enhancement of $\tilde{P}(q = \pi, \tau = 400/t)$ for small A_0 is essentially determined by the first-order perturbation theory with $\cos A(\tau) \approx 1$. Indeed, the ω_p dependence of $\tilde{P}(q = \pi, \tau = 400/t)$ for large A_0 no longer follows $\chi(\omega)$ and the broad enhancement of the η-pairing correlation is found in a range of $0.3t \lesssim \omega_p \lesssim 4t$.

C. Distribution of η-pairing eigenstates

To investigate the distribution of η-pairing eigenstates in the photoexcited state $|\psi(\tau)\rangle$, let us calculate the spectral function $P(\eta, \omega, \tau)$ given by

$$P(\eta, \omega, \tau) = \langle\psi(\tau)|\hat{\mathcal{E}}_\delta(\eta)\delta_\varepsilon(\omega - \hat{\mathcal{H}} + E_0)\hat{\mathcal{E}}_\delta(\eta)|\psi(\tau)\rangle, \qquad (78)$$

where $\hat{\mathcal{E}}_\delta(\eta)$ is the projection operator onto the subspace with a given value of η, i.e.,

$$\hat{\mathcal{E}}_\delta(\eta) = \exp[-(\hat{\boldsymbol{\eta}}^2 - \eta(\eta+1))^2/\delta^2] \qquad (79)$$

in the limit of $\delta \to 0$. For a practical value of δ in the numerical calculations, we set δ as small as $1/\sqrt{5}$. The detail of the numerical implementation is described in the Appendix.

Figure 4 shows typical results of the spectral function $P(\eta, \omega, \tau)$ calculated at $\tau = 400/t$. We find that finite intensities appear at $\omega \sim 2n\omega_p$ for η even and $\omega \sim (2n+1)\omega_p$ for η odd, where n is non-negative integer. This is in good accordance with the result for the time-dependent perturbation theory described in Sec. II E. Notice that the finite contribution with $\eta > 1$ cannot be explained by the first-order perturbation process since the rank-1 tensor operator can change the value of η by 1, indicating the importance of the nonlinear processes. These eigenstates with η finite are responsible for the enhancement of the η-pairing correlation in the photoinduced state.

D. Dynamical spin correlation

To examine the effects of the photoinduced η pairs on the localized spins, here we calculate the dynamical correlation function for the localized spins defined as

$$M_{j'j}(\tau', \tau) = \langle\psi(\tau)|\hat{M}_{j'}^z(\tau')\hat{M}_j^z|\psi(\tau)\rangle, \qquad (80)$$

where

$$\hat{M}_j^z(\tau) = e^{i\hat{\mathcal{H}}\tau}\hat{M}_j^z e^{-i\hat{\mathcal{H}}\tau}. \qquad (81)$$

Here, $M_{j'j}(\tau', \tau)$ is a quantity indicating how the spin $\hat{M}_j^z$ for the state $|\psi(\tau)\rangle$ is correlated to the spin $\hat{M}_{j'}^z$ after the time τ'. Figures 5(a) and 5(c) show the results of $M_{j'j}(\tau', \tau)$ for the initial state at $\tau = 0$, which is the ground state of the half-filled 1D Kondo lattice model $\hat{\mathcal{H}}$. Recalling that the
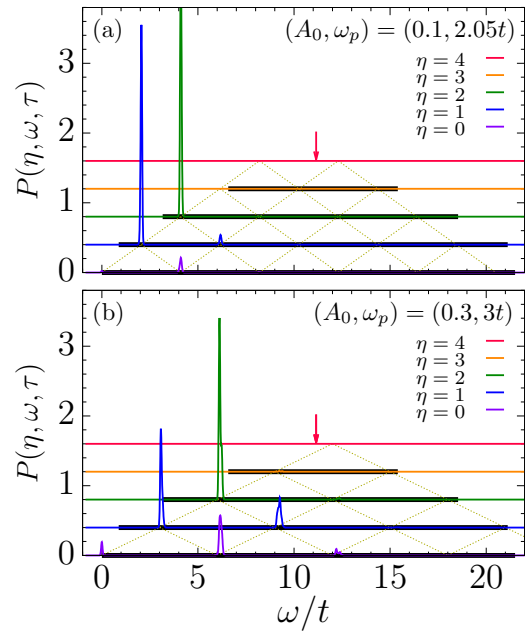

FIG. 4. Spectral function $P(\eta, \omega, \tau)$ in the photoexcited state $|\psi(\tau)\rangle$ at $\tau = 400/t$ for the half-filled 1D Kondo lattice model with $J = t$ and $L = 8$ under the external field $A(\tau)$ with (a) $A_0 = 0.1$ and $\omega_p = 2.05t$, and (b) $A_0 = 0.3$ and $\omega_p = 3t$. The other parameters for $A(\tau)$ are $\tau_c = 200/t$ and $\tau_\omega = 50/t$. For visibility, the spectral functions with different values of η are shifted vertically. Black solid lines indicate the energy region where the eigenstates of $\hat{\mathcal{H}}$ exist for each η. Red arrows indicate the excitation energy of the vacuum state $|vac\rangle$. Crossing points between dashed lines and black solid lines indicate $\omega = 2n\omega_p$ for η even and $\omega = (2n+1)\omega_p$ for η odd, where $n = 0, 1, 2, \ldots$.

ground state is an insulating state with a finite spin gap due to the formation of local singlets, the low-lying spin excitations are described by the triplonlike excitations similar to the excitations in the valence bond solids [32–34]. In the Kondo lattice model, the triplon is a local object composed of a conduction electron and a localized spin, and this picture is more preferable for large J/t because for a small or moderate value of J/t the triplon is likely a spatially more extended object. Therefore, in a small J/t region, we expect the spin excitations similar to those found in the case where the antiferromagnetic correlation is dominant. However, these different behaviors are not distinguishable in our simulation using the limited size of clusters. Instead, we only find in Fig. 5(a) that the correlation is antiferromagnetic at $\tau' = 0$ and starts to oscillate gradually from the nearest to distant sites, which is characteristics for the ballistic dynamics in systems with strong antiferromagnetic correlation.

In contrast, we find in Figs. 5(b) and 5(d) that $M_{j'j}(\tau', \tau)$ after the pulse irradiation behaves more diffusive. The dynamical correlations not only for the same site $j = j'$ but also for the distant sites decrease in time, and the oscillatory behavior is no longer remarkable. Such a diffusive nature indicates the softening of the spectral function because the diffusive nature suggests a quadratic form of the energy dispersion with respect to momentum. In Fig. 5(c), we display the frequency-dependent dynamical correlation function $\tilde{M}_{jj}(\omega, \tau)$ obtained
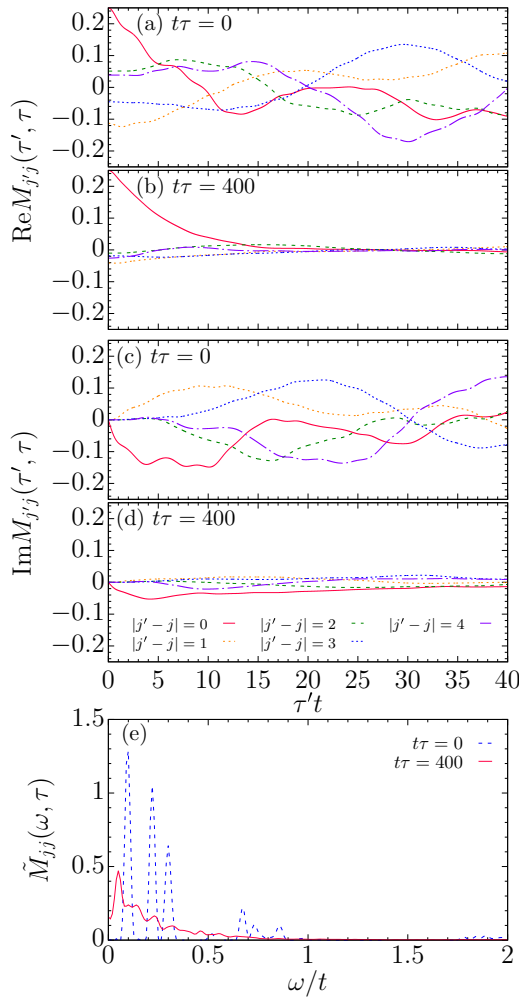
FIG. 5. (a), (b) Real part of dynamical correlation functions $M_{j'j}(\tau', \tau)$ for (a) the initial state at $\tau = 0$ and (b) the time-evolved state after the pulse irradiation at $\tau = 400/t$. (c), (d) Imaginary part of $M_{j'j}(\tau', \tau)$ for (c) the initial state $\tau = 0$ and (d) the time-evolved state after the pulse irradiation at $\tau = 400/t$. (e) Frequency-dependent dynamical correlation function $\tilde{M}_{jj}(\omega, \tau)$ at $\tau = 0$ and $400/t$. The results are obtained for the half-filled 1D Kondo lattice model with $J = t$ and $L = 8$ under the external field $A(\tau)$ with $A_0 = 0.38$, $\omega_p = 3/t$, $\tau_w = 50/t$, and $\tau_c = 200/t$.

by the Fourier transform of $M_{jj}(\tau', \tau)$, i.e.,

$$\tilde{M}_{jj}(\omega, \tau) = \frac{1}{T} \int_0^T d\tau' g(\tau') M_{jj}(\tau', \tau) e^{i\omega\tau'}, \quad (82)$$

where we set $T = 200/t$ and multiply the integrand by a contour $g(\tau) = (1 + \cos(\pi \tau / T))/2$ which makes delta peaks broad, for obtaining a smooth function [35]. We find that the main peaks in $\tilde{M}_{jj}(\omega, \tau)$ after the pulse irradiation at $\tau = 400/t$ shift to lower energies as compared to the spectrum before the pulse irradiation at $\tau = 0$.

The diffusive behavior of the dynamical spin correlation function is understood as a consequence of the generation of η pairs, which leads to the decoupling between the localized spins and the mobile electrons, as discussed for Yang's state in Sec. II B. Here, we show that this picture is related to the photodoping mechanism [36–40]. To this end, we introduce

$|\phi_{\alpha, \eta, \eta_z}\rangle$ being a state for (η, η_z) sector to decompose the photoexcited state $|\psi(\tau)\rangle$ as

$$|\psi(\tau)\rangle = \sum_{\alpha, \eta} c_{\alpha\eta}(\tau) |\phi_{\alpha, \eta, \eta_z}\rangle, \quad (83)$$

where index α is introduced to distinguish states with the same value of η. Note that η_z is fixed to be zero at half filling. Let $M_{jj'}^{(\alpha, \eta, \eta_z),(\alpha', \eta', \eta_z')}(\tau')$ be the dynamical correlation function defined by

$$M_{j'j}^{(\alpha, \eta, \eta_z),(\alpha', \eta', \eta_z')}(\tau') = \langle \phi_{\alpha, \eta, \eta_z} | \hat{M}_{j'}^z(\tau') \hat{M}_j^z | \phi_{\alpha', \eta', \eta_z'} \rangle. \quad (84)$$

Notice that $|\phi_{\alpha, \eta, \eta_z}\rangle$ is not necessarily an energy eigenstate of $\hat{\mathcal{H}}$ but an eigenstate of $\hat{\eta}^2$ and $\hat{\eta}_z$. Since $\hat{\eta}^+$ and $\hat{\eta}^-$ commute with $\hat{M}_i^z$ as well as $\hat{\mathcal{H}}$, $\hat{M}_j^z(\tau') \hat{M}_j^z$ is considered as a rank-0 tensor operator for the pseudospin operators $\hat{\eta}_\mu$ ($\mu = x, y, z$). Therefore, applying the Wigner-Eckert theorem in Eq. (40), we obtain

$$M_{j'j}^{(\alpha, \eta, \eta_z),(\alpha', \eta', \eta_z')}(\tau') = \delta_{\eta, \eta'} \delta_{\eta_z, \eta_z'} M_{j'j}^{(\alpha, \eta, -\eta),(\alpha', \eta, -\eta)}(\tau') \quad (85)$$

because

$$\langle \eta, \eta_z 00 | \eta' \eta_z' \rangle = \delta_{\eta, \eta'} \delta_{\eta_z, \eta_z'}. \quad (86)$$

Equation (85) suggests that the dynamical spin correlation function $M_{j'j}^{(\alpha, \eta, \eta_z),(\alpha', \eta', \eta_z)}(\tau')$ for electron number $N = L + 2\eta_z$ exactly coincides to that for $N = L - 2\eta$. Note that $|\phi_{\alpha, \eta, \eta_z = -\eta}\rangle$ is a lowest weight state [41] because $\hat{\eta}^- |\phi_{\alpha, \eta, -\eta}\rangle = 0$, implying that there are no η pairs in $|\phi_{\alpha, \eta, -\eta}\rangle$. Moreover, by using Eq. (85), the dynamical spin correlation function after the pulse irradiation can be represented as

$$M_{j'j}(\tau', \tau) = \sum_{\alpha, \alpha', \eta} c_{\alpha\eta}^*(\tau) c_{\alpha'\eta}(\tau) M_{j'j}^{(\alpha, \eta, -\eta),(\alpha', \eta, -\eta)}(\tau'), \quad (87)$$

suggesting that the spin dynamical correlation function at half filling (i.e., $\eta_z = 0$) can be represented as a simple sum of the spin dynamical correlation functions for the hole-doped systems.

We thus find that the photogeneration of η pairs is inseparably related to photodoping when we consider the spin dynamics. This is expected because the energy eigenstate with quantum number $\eta = -\eta_z = \frac{1}{2}(N - 2N_\eta - L)$ span the subspace of the $N - 2N_\eta$ electron system and the multiplication of $\hat{\eta}^+$ operator by N_η times to this state replaces N_η empty sites with doubly occupied sites, which is an energy eigenstate with N electrons, having the same energy eigenvalue, and does not affect the properties of spin degrees of freedom. Considering that the ground state of the 1D Kondo lattice model varies from a paramagnetic phase to a ferromagnetic phase with increasing the hole concentration [42], we can understand that the photogeneration of η pairs, which is essentially the *in situ* doping, changes drastically the spin dynamics of the initial ground state at half filling.

Finally, we also notice in Fig. 5(b) that the equal-time correlation $M_{j'j}(\tau' = 0, \tau)$ is less dependent on the distance $|j' - j| (\neq 0)$. This tendency is explained by the dephasing mechanism recently proposed in Ref. [43]. This mechanism states that in a system with SU(2)×SU(2) symmetry, e.g, having both spin and η-SU(2) symmetries, if we apply a Floquet-type time-dependent perturbation that commutes with

one of the SU(2) symmetries but breaks the other symmetry, the correlation function composed of the local operators represented by generators of the SU(2) symmetry that commutes with the perturbation becomes spatially uniform in a steady state. For example, in Ref. [43], they have demonstrated in the Hubbard model that by applying the time-dependent perturbation $h(\tau) \sum_j \hat{S}_j^z$, the correlation function $\langle \hat{c}_{j\downarrow} \hat{c}_{j\uparrow} \hat{c}_{j'\uparrow}^\dagger \hat{c}_{j'\downarrow}^\dagger \rangle$ in a steady state becomes spatially uniform. Notice that $h(\tau) \sum_j \hat{S}_j^z$ breaks the spin-SU(2) symmetry and changes the quantum number of the total spin, but commutes with $\hat{c}_{j\downarrow} \hat{c}_{j\uparrow}$. This dephasing mechanism can be applied to our case. The time-dependent perturbation is $\hat{\mathcal{V}}(\tau)$ that breaks the η-SU(2) symmetry and changes the quantum number of $\hat{\eta}^2$, but commutes with $\hat{M}_j^z$. Therefore, the correlation function $M_{jj'}(\tau' = 0, \tau)$ becomes spatially uniform in a steady state, as found in Fig. 5(b). We should note that the discussion given above is not limited for the localized spins but is also applied to the electron spins in the conduction band.

IV. SUMMARY AND DISCUSSION

By using the time-dependent exact diagonalization technique, we have shown that the pulse irradiation can generate η pairs and thus induce the enhancement of the pair-density-wave-like superconducting correlation in the ground state of the 1D Kondo lattice model at half filling. The η-pairing states are preferentially generated by the optical field because of the symmetry associated with the η-pairing operators $\hat{\boldsymbol{\eta}} = (\hat{\eta}_x, \hat{\eta}_y, \hat{\eta}_z)$ that satisfy the SU(2) commutation relations. This was also analytically shown using the time-dependent perturbation theory, by which the selection rule becomes apparent. We have furthermore investigated the effect on the localized spin degrees of freedom in the photoexcited state and found that the spin dynamics becomes diffusive after the pulse irradiation. This is understood because the generation of η pairs decouple locally the exchange interaction, which is essentially equivalent to the effective hole doping.

The numerical simulation in Sec. III is for the 1D Kondo lattice model with the antiferromagnetic exchange interaction. However, the symmetry analysis given in Sec. II is applicable for any spatial dimension as long as the system is bipartite. It is also obvious that the sign of the exchange interaction does not affect the discussion in Sec. II. Moreover, since the pseudospin operators $\hat{\boldsymbol{\eta}} = (\hat{\eta}_x, \hat{\eta}_y, \hat{\eta}_z)$ are defined only for the mobile electrons, the symmetry analysis given in Sec. II is still correct even when we add any exchange interaction term between the localized spins,

$$\sum_{j,j'} \bar{J}_{jj'} \hat{\boldsymbol{M}}_j \cdot \hat{\boldsymbol{M}}_{j'}, \tag{88}$$

which are not necessarily in the bipartite structure. Therefore, we can prepare various initial states with different spin structures, including the Haldane phase in the 1D system with $J < 0$ as well as a quantum spin liquid for the frustrated exchange coupling $\bar{J}_{jj'}$. We have implicitly assumed that the localized spins $\hat{\boldsymbol{M}}_j$ are spin 1/2. However, this assumption is not necessary for the symmetry analysis in Sec. II. The η-pairing operators $\hat{\boldsymbol{\eta}} = (\hat{\eta}_x, \hat{\eta}_y, \hat{\eta}_z)$ and the η-pairing states

are still well defined even when we consider the Kondo lattice model with the classical localized spins.

Another model related to this study is the periodic Anderson model described by the following Hamiltonian:

$$\hat{\mathcal{H}}_{\text{PA}} = \hat{\mathcal{H}}_t + \hat{\mathcal{H}}_V + \hat{\mathcal{H}}_U, \tag{89}$$

where

$$\hat{\mathcal{H}}_V = V \sum_j \sum_{\sigma=\uparrow,\downarrow} (\hat{c}_{j\sigma}^\dagger \hat{d}_{j\sigma} + \hat{d}_{j\sigma}^\dagger \hat{c}_\sigma) \tag{90}$$

and

$$\hat{\mathcal{H}}_U = U \sum_j \left(\hat{d}_{j\uparrow}^\dagger \hat{d}_{j\uparrow} - \frac{1}{2} \right) \left(\hat{d}_{j\downarrow}^\dagger \hat{d}_{j\downarrow} - \frac{1}{2} \right). \tag{91}$$

Here, $\hat{\mathcal{H}}_t$ is defined in Eq. (2) and $\hat{d}_{j\sigma}$ ($\hat{d}_{j\sigma}^\dagger$) denotes the annihilation (creation) operator of a localized electron with spin σ ($=\uparrow, \downarrow$) at site j. It is well known that the Kondo lattice model is the effective low-energy model of the periodic Anderson model in the limit of $U \to \infty$. We should note that, in this case, the η-pairing operators $\hat{\boldsymbol{\eta}} = (\hat{\eta}_x, \hat{\eta}_y, \hat{\eta}_z)$ defined in Eqs. (7)–(9) do not commute with $\hat{\mathcal{H}}_{\text{PA}}$, but their definition has to be extended as follows:

$$\hat{\eta}_x^{\text{(PA)}} = \hat{\eta}_x - \frac{1}{2} \sum_j e^{i\phi_j} (\hat{d}_{j\uparrow}^\dagger \hat{d}_{j\downarrow}^\dagger + \hat{d}_{j\downarrow} \hat{d}_{j\uparrow}), \tag{92}$$

$$\hat{\eta}_y^{\text{(PA)}} = \hat{\eta}_y - \frac{1}{2i} \sum_j e^{i\phi_j} (\hat{d}_{j\uparrow}^\dagger \hat{d}_{j\downarrow}^\dagger - \hat{d}_{j\downarrow} \hat{d}_{j\uparrow}), \tag{93}$$

$$\hat{\eta}_z^{\text{(PA)}} = \hat{\eta}_z + \frac{1}{2} \sum_j (\hat{d}_{j\uparrow}^\dagger \hat{d}_{j\uparrow} + \hat{d}_{j\downarrow}^\dagger \hat{d}_{j\downarrow} - 1). \tag{94}$$

Notice that these operators satisfy the SU(2) commutation relations and commute with $\hat{\mathcal{H}}_{\text{PA}}$ for any U, including the case when U is negative.

The negative-U periodic Anderson model has been considered to discuss the charge Kondo effect for materials containing valence skipping elements [44]. The strong coupling limit of the negative-U periodic Anderson model is described by the charge Kondo lattice model:

$$\hat{\mathcal{H}}_{c\text{KL}} = \hat{\mathcal{H}}_t + \hat{\mathcal{H}}_{\bar{J}}, \tag{95}$$

where

$$\hat{\mathcal{H}}_{\bar{J}} = \bar{J} \sum_j \hat{\boldsymbol{\eta}}_j \cdot \hat{\boldsymbol{\eta}}_{jd}. \tag{96}$$

Here, $\hat{\boldsymbol{\eta}}_j = (\hat{\eta}_j^x, \hat{\eta}_j^y, \hat{\eta}_j^z)$ and $\hat{\boldsymbol{\eta}}_{jd} = (\hat{\eta}_{jd}^x, \hat{\eta}_{jd}^y, \hat{\eta}_{jd}^z)$ represent the local η-pairing operators for the conduction and localized electrons, respectively, given by

$$\hat{\eta}_j^x = \frac{1}{2} e^{i\phi_j} (\hat{c}_{j\uparrow}^\dagger \hat{c}_{j\downarrow}^\dagger + \hat{c}_{j\downarrow} \hat{c}_{j\uparrow}), \tag{97}$$

$$\hat{\eta}_j^y = \frac{1}{2i} e^{i\phi_j} (\hat{c}_{j\uparrow}^\dagger \hat{c}_{j\downarrow}^\dagger - \hat{c}_{j\downarrow} \hat{c}_{j\uparrow}), \tag{98}$$

$$\hat{\eta}_j^z = \frac{1}{2} (\hat{c}_{j\uparrow}^\dagger \hat{c}_{j\uparrow} + \hat{c}_{j\downarrow}^\dagger \hat{c}_{j\downarrow} - 1), \tag{99}$$

and

$$\hat{\eta}_{jd}^x = -\frac{1}{2} e^{i\phi_j} (\hat{d}_{j\uparrow}^\dagger \hat{d}_{j\downarrow}^\dagger + \hat{d}_{j\downarrow} \hat{d}_{j\uparrow}), \tag{100}$$

$$\hat{\eta}_{jd}^y = -\frac{1}{2i}e^{i\phi_j}(\hat{d}_{j\uparrow}^\dagger \hat{d}_{j\downarrow}^\dagger - \hat{d}_{j\downarrow}\hat{d}_{j\uparrow}), \tag{101}$$

$$\hat{\eta}_{jd}^z = \frac{1}{2}(\hat{d}_{j\uparrow}^\dagger \hat{d}_{j\uparrow} + \hat{d}_{j\downarrow}^\dagger \hat{d}_{j\downarrow} - 1), \tag{102}$$

and $\tilde{J} = 8V^2/|U|$. Notice that these local η-pairing operators also satisfy the SU(2) commutation relations among themselves, i.e., $[\hat{\eta}_j^\mu, \hat{\eta}_{j'}^\nu] = i\delta_{jj'}\sum_\lambda \varepsilon_{\mu\nu\lambda}\hat{\eta}_j^\lambda$ and $[\hat{\eta}_{jd}^\mu, \hat{\eta}_{j'd}^\nu] = i\delta_{jj'}\sum_\lambda \varepsilon_{\mu\nu\lambda}\hat{\eta}_{jd}^\lambda$. In this case, even although the total charge of the conduction electrons fluctuates, the extended η-pairing operators in Eqs. (92)–(94) still commute with the charge Kondo lattice Hamiltonian $\hat{\mathcal{H}}_{cKL}$.

The photoexcitation of these systems are highly interesting and the research along this line is now in progress.

APPENDIX: TECHNICAL DETAILS OF NUMERICAL CALCULATIONS

This Appendix summarizes the numerical methods to calculate the dynamical current correlation function $\chi(\omega)$ in Eq. (75) and the spectral function $P(\eta, \omega, \tau)$ in Eq. (78).

Let us first describe the method to calculate the following projected state:

$$|\psi_\eta(\tau)\rangle = \hat{\mathcal{E}}_\delta(\eta)|\psi(\tau)\rangle, \tag{A1}$$

which appears in Eq. (78). We first divide the exponential operator $\hat{\mathcal{E}}_\delta(\eta)$ in Eq. (79) into many slices:

$$\hat{\mathcal{E}}_\delta(\eta) = [\hat{\mathcal{E}}_{\sqrt{M}\delta}(\eta)]^M. \tag{A2}$$

We then multiply $\hat{\mathcal{E}}_{\sqrt{M}\delta}(\eta)$ sequentially to $|\psi(\tau)\rangle$ as

$$|v_m\rangle = \hat{\mathcal{E}}_{\sqrt{M}\delta}(\eta)|v_{m-1}\rangle \tag{A3}$$

for $m = 1, 2, \ldots, M$ with

$$\begin{aligned} |v_0\rangle &= |\psi(\tau)\rangle, \\ |v_M\rangle &= |\psi_\eta(\tau)\rangle. \end{aligned} \tag{A4}$$

At each step of m, we use the Taylor expansion of the exponential operator $\hat{\mathcal{E}}_{\sqrt{M}\delta}(\eta)$, similar to the case for the time-evolution operator in Eqs. (68)–(70). We find that this is numerically stable for any case studied here.

Next, we should notice that the dynamical current correlation function $\chi(\omega)$ and the spectral function $P(\eta, \omega, \tau)$ have the following form:

$$S(\omega) = \langle\psi|\delta_\varepsilon(\hat{\mathcal{H}} - \omega + E_0)|\psi\rangle, \tag{A5}$$

where $|\psi\rangle = \hat{\mathcal{J}}|\psi(0)\rangle$ for $\chi(\omega)$ and $|\psi\rangle = \hat{\mathcal{E}}_\delta(\eta)|\psi(\tau)\rangle$ for $P(\eta, \omega, \tau)$. To calculate $S(\omega)$, we use the following formula:

$$S(\omega) = \frac{1}{\sqrt{2\pi\varepsilon^2}}\sum_{k=1}^K e^{-(\xi_k-\omega+E_0)^2/2\varepsilon^2}|\langle e_1|\xi_k\rangle|^2. \tag{A6}$$

Here, $|e_k\rangle$ with $k = 1, 2, \ldots, K$ is a set of the orthonormalized bases (i.e., $\langle e_k|e_{k'}\rangle = \delta_{k,k'}$) generated by the Lanczos procedure

$$\begin{aligned} |e_1\rangle &= |\psi\rangle, \\ \beta_1|e_2\rangle &= \hat{\mathcal{H}}|e_1\rangle - \alpha_1|e_1\rangle, \\ \beta_k|e_{k+1}\rangle &= \hat{\mathcal{H}}|e_k\rangle - \alpha_k|e_k\rangle - \beta_{k-1}|e_{k-1}\rangle \quad (\text{for } k \geqslant 2), \end{aligned} \tag{A7}$$

where $\alpha_k = \langle e_k|\hat{\mathcal{H}}|e_k\rangle$. Notice that the coefficients α_k and β_k correspond to the matrix elements of Hamiltonian $\hat{\mathcal{H}}$ taken in the reduced Hilbert space spanned by the basis set $\{|e_k\rangle\}$. ξ_k and $|\xi_k\rangle$ with $k = 1, 2, \ldots, K$ in Eq. (A6) are the approximate eigenvalues and eigenstates of $\hat{\mathcal{H}}$, respectively, obtained by diagonalizing the tridiagonal matrix constructed via the Lanczos iteration in Eqs. (A7). Note that $\langle e_1|\xi_k\rangle$ is the first element of $|\xi_k\rangle$ represented in the basis set of $\{|e_k\rangle\}$. ξ_k yields the peak positions in the spectral function $S(\omega)$, which coincide with the pole positions obtained by the continued fraction technique [45].

[1] Y. Tokura, J. Phys. Soc. Jpn. **75**, 011001 (2006).

[2] S. Iwai and H. Okamoto, J. Phys. Soc. Jpn. **75**, 011007 (2006).

[3] C. Giannetti, M. Capone, D. Fausti, M. Fabrizio, F. Parmigiani, and D. Mihailovic, Adv. Phys. **65**, 58 (2016).

[4] D. Fausti, R. I. Tobey, N. Dean, S. Kaiser, A. Dienst, M. C. Hoffmann, S. Pyon, T. Takayama, H. Takagi, and A. Cavalleri, Science **331**, 189 (2011).

[5] W. Hu, S. Kaiser, D. Nicoletti, C. R. Hunt, I. Gierz, M. C. Hoffmann, M. Le Tacon, T. Loew, B. Keimer, and A. Cavalleri, Nat. Mater. **13**, 705 (2014).

[6] S. Kaiser, C. R. Hunt, D. Nicoletti, W. Hu, I. Gierz, H. Y. Liu, M. Le Tacon, T. Loew, D. Haug, B. Keimer, and A. Cavalleri, Phys. Rev. B **89**, 184516 (2014).

[7] M. Mitrano, A. Cantaluppi, D. Nicoletti, S. Kaiser, A. Perucchi, S. Lupi, P. Di Pietro, D. Pontiroli, M. Riccò, S. R. Clark, D. Jaksch, and A. Cavalleri, Nature **530**, 461 (2016).

[8] A. Cantaluppi, M. Buzzi, G. Jotzu, D. Nicoletti, M. Mitrano, D. Pontiroli, M. Riccò, A. Perucchi, P. Di Pietro, and A. Cavalleri, Nat. Phys. **14**, 837 (2018).

[9] S. Iwai, M. Ono, A. Maeda, H. Matsuzaki, H. Kishida, H. Okamoto, and Y. Tokura, Phys. Rev. Lett. **91**, 057401 (2003).

[10] H. Okamoto, H. Matsuzaki, T. Wakabayashi, Y. Takahashi, and T. Hasegawa, Phys. Rev. Lett. **98**, 037401 (2007).

[11] H. Uemura, H. Matsuzaki, Y. Takahashi, T. Hasegawa, and H. Okamoto, J. Phys. Soc. Jpn. **77**, 113714 (2008).

[12] H. Okamoto, T. Miyagoe, K. Kobayashi, H. Uemura, H. Nishioka, H. Matsuzaki, A. Sawa, and Y. Tokura, Phys. Rev. B **82**, 060513(R) (2010).

[13] H. Okamoto, T. Miyagoe, K. Kobayashi, H. Uemura, H. Nishioka, H. Matsuzaki, A. Sawa, and Y. Tokura, Phys. Rev. B **83**, 125102 (2011).

[14] K. Yonemitsu and K. Nasu, Phys. Rep. **465**, 1 (2008).

[15] H. Aoki, N. Tsuji, M. Eckstein, M. Kollar, T. Oka, and P. Werner, Rev. Mod. Phys. **86**, 779 (2014).

[16] S. Ishihara, J. Phys. Soc. Jpn. **88**, 072001 (2019).

[17] T. Oka and S. Kitamura, Annu. Rev. Condens. Matter Phys. **10**, 387 (2019).

[18] T. Kaneko, T. Shirakawa, S. Sorella, and S. Yunoki, Phys. Rev. Lett. **122**, 077002 (2019).

[19] C. N. Yang, Phys. Rev. Lett. **63**, 2144 (1989).

[20] R. Fujiuchi, T. Kaneko, Y. Ohta, and S. Yunoki, Phys. Rev. B **100**, 045121 (2019).

[21] T. Kaneko, S. Yunoki, and A. J. Millis, arXiv:1910.11229.

[22] H. Tsunetsugu, M. Sigrist, and K. Ueda, Rev. Mod. Phys. **69**, 809 (1997).

[23] D. L. Cox and A. Zawadowski, Adv. Phys. **47**, 599 (1998).

[24] J. J. Sakurai, *Modern Quantum Mechanics* (Addison-Wesley, Reading, MA, 1994).

[25] S. Kitamura and H. Aoki, Phys. Rev. B **94**, 174503 (2016).

[26] H. Tsunetsugu, Y. Hatsugai, K. Ueda, and M. Sigrist, Phys. Rev. B **46**, 3175 (1992).

[27] C. C. Yu and S. R. White, Phys. Rev. Lett. **71**, 3866 (1993).

[28] A. M. Tsvelik, Phys. Rev. Lett. **72**, 1048 (1994).

[29] S. Fujimoto and N. Kawakami, J. Phys. Soc. Jpn. **66**, 2157 (1997).

[30] F. F. Assaad, Phys. Rev. Lett. **83**, 796 (1999).

[31] The pulse described by this external field $A(\tau)$ has the pulse width (full width at half maximum) of approximately 150 fs and introduces the time-dependent electric field $E(\tau) = -\partial A(\tau)/\partial \tau$ with the maximum electric field as large as 2 MV/;cm, assuming that $t = 0.5$ eV and a lattice constant $a = 5$ Å.

[32] S. Sachdev and R. N. Bhatt, Phys. Rev. B **41**, 9323 (1990).

[33] S. Gopalan, T. M. Rice, and M. Sigrist, Phys. Rev. B **49**, 8901 (1994).

[34] C. Jurecka and W. Brenig, Phys. Rev. B **64**, 092406 (2001).

[35] L. Wang and H.-Q. Lin, arXiv:1901.07751.

[36] N. Maeshima and K. Yonemitsu, J. Phys. Soc. Jpn. **74**, 2671 (2005).

[37] P. Werner, H. U. R. Strand, S. Hoshino, Y. Murakami, and M. Eckstein, Phys. Rev. B **97**, 165119 (2018).

[38] P. Werner, J. Li, D. Golež, and M. Eckstein, Phys. Rev. B **100**, 155130 (2019).

[39] P. Werner, M. Eckstein, M. Müller, and G. Refael, Nat. Commun. **10**, 5556 (2019).

[40] J. Li, D. Golez, P. Werner, and M. Eckstein, arXiv:1908.08693.

[41] F. H. Essler, H. Frahm, F. Göhmann, A. Klümper, and V. E. Korepin, *The One-Dimensional Hubbard Model* (Cambridge University Press, Cambridge, 2005).

[42] H. Tsunetsugu, M. Sigrist, and K. Ueda, Phys. Rev. B **47**, 8345 (1993).

[43] J. Tindall, B. Buča, J. R. Coulthard, and D. Jaksch, Phys. Rev. Lett. **123**, 030603 (2019).

[44] H. Matsuura and K. Miyake, J. Phys. Soc. Jpn. **81**, 113705 (2012).

[45] E. Dagotto, Rev. Mod. Phys. **66**, 763 (1994).